THE INFLUENCE OF SPECIMENS PREPARATION METHOD ON COHESIVE BEHAVIOR OF FIBER COMPOSITES

Michal Přinosil*, Petr Kabele*

The correct determination of material properties of construction materials from experiments is important not only during their development, but also during final verification. Specimens for testing mechanical properties of fiber-reinforced composites with a quasi-brittle matrix are usually prepared by casting into a suitable mold. But they can be also prepared by cutting to desired shape from large body of material. The method of preparation may affect the measured values of material characteristics. In the case of sawed specimens, the fibers in surface layer are damaged, while in the case of casted specimens, fibers in surface layer tended to align with mold surface. The purpose of this article is to clarify the influence of these phenomena using numerical simulations.

Keywords : *fiber-reinforced composites, fiber bridging, cohesive law, specimens preparation method*

1. Introduction

Historical monuments are part of every advanced civilization. To preserve these objects, suitable maintenance and protection is required. Within restoration works, it is necessary to respect their origin and character. This applies in particular the use of the most appropriate materials, that are also compatible (chemical, physical, mechanical) with the original. In our research, we are developing a new high performance lime-based fiber-reinforced mortar for restoration works on historical structures. Application of the mortar is intended in places, where the mortar in masonry failures and cracks due to extensive strains (volume changes, imposed deformations due to foundation movements etc.).

The correct determination of mechanical characteristics is decisive for the design of the mortar composition. Characteristics can be evaluated from the data from experiments or from the numerical simulations of these experiments. The effort of researches is that the preparation of experiment doesn't affect the measured data. It is always not possible to avoid these effects. In the case of fiber composites, the results can be affected by manufacturing process of experimental specimens. The aim of this study is to clarify the differences in behavior between specimens prepared by casting into a suitable mold and sawed from a larger body of material. For this purpose, numerical simulations for prediction of cohesive relationship of fiber composites specimens prepared both techniques were performed.

* Ing. M. Přinosil, prof. Ing. P. Kabele, Ph.D., Czech Technical University in Prague, Faculty of Civil Engineering, Department of Mechanics, Thákurova 7, 166 29 Prague, CZ

2. Behavior of a single fiber

The cohesive behavior of the crack of fiber composites is connected to behavior of a single fiber during extraction from the surrounding matrix. This process can be described by the relationship between applied force P and the displacement u of the pulled end of the fiber. In our model we use the description, which the process divides into two separate stages [1], [2].

When a crack forms, a crack-bridging fiber is activated. Opening of the crack causes an increasing force in the fiber, which corresponds to the chemical bond G_d. After exhausting, the fiber debonds from the matrix and the debonded part of the fiber elastically stretches, which is prevented by frictional stress τ_0 on the interface. The debonding stage can be described by the equation:

$$P_\mathrm{deb} = \sqrt{\frac{\pi^2\, \tau_0\, E_\mathrm{f}\, d_\mathrm{f}^2}{2}\, u + \frac{\pi^2\, G_\mathrm{d}\, E_\mathrm{f}\, d_\mathrm{f}^3}{2}}\ , \tag{1}$$

where d_f is the fiber diameter, E_f is its Young's modulus of elasticity. The debonding finishes when the debonded length reaches the embedment end of the fiber. The corresponding displacement of the pulled end of the fiber with embedment length L_e is:

$$\delta_\mathrm{c} = \frac{2\, \tau_0\, L_\mathrm{e}^2}{E_\mathrm{f}\, d_\mathrm{f}} + \sqrt{\frac{8\, G_\mathrm{d}\, L_\mathrm{e}^2}{E_\mathrm{f}\, d_\mathrm{f}}}\ . \tag{2}$$

With increasing displacement u the fiber starts slips out from the matrix with decreasing contact area:

$$P_\mathrm{pull} = \pi\, d_\mathrm{f}\, \tau_0 \left(1 + \frac{\beta\,(u - \delta_\mathrm{c})}{d_\mathrm{f}}\right)(L_\mathrm{e} - u - \delta_\mathrm{c})\ . \tag{3}$$

The parameter β controls whether the pull-out stage has linear decreasing character, or if there is hardening or softening (due to abrasion of the fiber, accumulation of loose particles of the matrix, etc.).

When the fiber is not perpendicular to the crack plane (there is angle φ between normal to the crack plane and the fiber axis), the force in the fiber is:

$$P(\varphi) = P(0)\, \mathrm{e}^{f\varphi} \tag{4}$$

and its strength is:

$$f_\mathrm{t}(\varphi) = f_\mathrm{t}(0)\, \mathrm{e}^{-f'\varphi}\ , \tag{5}$$

where f is snubbing coefficient and f' is strength reduction coefficient.

3. Numerical simulations

Numerical simulations were performed to predict cohesive behavior of a single crack (cohesive law) – relation between crack opening displacement δ and bridging stress σ_b. As the material we consider lime-based mortar reinforced with polyvinyl-alcohol fibers (PVA – type REC 15, made by Kuraray Company) in volume fraction 2 % with variable length (4–12 mm). The micromechanical parameters used in Eq. (1)–(5) have been previously experimentally identified [3] and they are listed in Tab. 1.

Simulations were performed so that, first of all, fibers with uniform diameter and length were randomly generated in a prismatic volume. The size 40×40×160 mm corresponded to the standard beam, which we use for experiments. Secondly, at least ten fictional crack planes, perpendicular to the longitudinal axis, were inserted into each specimen with minimal mutual distance corresponding to the length of fiber L_f. For incrementally increasing prescribed crack opening displacement δ the bridging stress σ_b was calculated as the sum of all forces P in fibers bridging the crack (according Eq. (1)–(5)) divided by the crack area A_c [4]:

$$\sigma_b(\delta) = \frac{\sum P_i(\delta, \varphi)}{A_c} \ . \tag{6}$$

The crack opening displacement included the displacements u of the fiber on both sides of the crack [2]:

$$\delta = u_1 + u_2 \ . \tag{7}$$

Furthermore, the cross-sectional plane was divided into a regular grid (Fig. 2) with dimension d_x (1–40 mm) and the bridging stress σ_b^{kl} in every part (row k and column l) was:

$$\sigma_b^{kl}(\delta) = \frac{\sum P_i(\delta, \varphi)}{d_x^2} \ . \tag{8}$$

From calculated data the most important was maximum bridging stress σ_{mb}^{kl}:

$$\sigma_{mb}^{kl} = \max(\sigma_b^{kl}(\delta)) \ . \tag{9}$$

d_f [mm]	L_f [mm]	E_f [MPa]	f_t [MPa]	τ_0 [MPa]	G_d [J/m^2]	β [–]	f [–]	f' [–]
0.04	12	13950	630	0.79	0.006	0.367	0.5	0.3

Tab.1: The micromechanical parameters

3.1. Generating of fiber reinforcement

Random Cartesian coordinates X_c, Y_c, Z_c determine the position of the fiber's center of gravity, random spherical coordinates λ and θ determine its orientation (Fig. 1). Rectangular distribution of all random variables ensures uniform distribution of fibers in a specimen. Using the assumption that the fiber is straight we can calculate the Cartesian coordinates of both ends of the fiber.

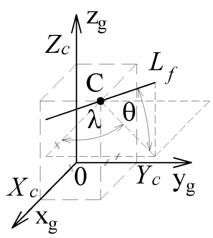

Fig.1: Position and orientation of a fiber determined by the random parameters

To reproduce the casted specimen, all fibers were generated in its volume. If any part of any fiber reached outside, coordinates of center of gravity remained fixed and only spherical coordinates were generated again until the condition was fulfilled. Therefore fibers in the surface layer tended to align with specimen surface. To reproduce the sawed specimen, fibers

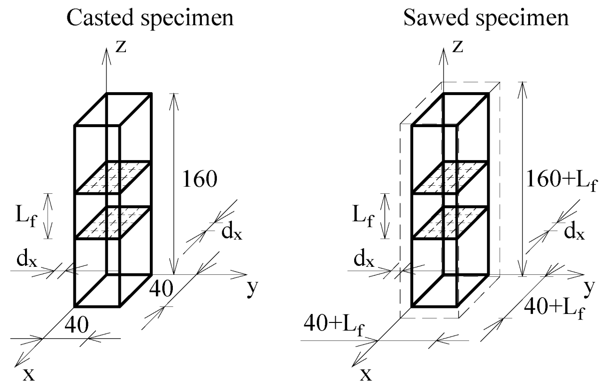

Fig.2: Schematic drawings of casted and sawed specimen

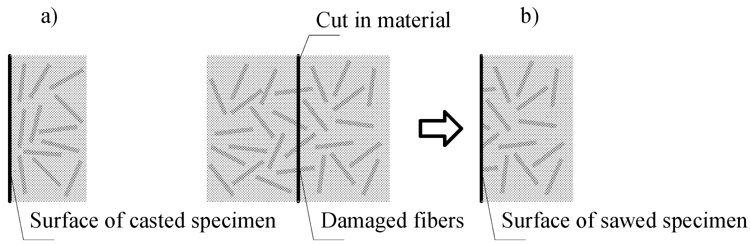

Fig.3: Surface layer in casted (a) and sawed (b) specimen

were generated in volume expanded on each side by one half of fiber's length (total amount of fibers was higher than in the casted specimen). Subsequently, only the parts of fibers in original volume (not expanded) were selected. Therefore fibers in the surface layer of the specimen could be broken (Fig. 3).

4. Effects of specimens preparation method

Typical calculated cohesive relations $\sigma_b(\delta)$ over the whole cross-sectional plane ($d_x =$ $= 40$ mm) of lime mortar reinforced with 2 % PVA fibers with length 12 mm for specimens with dimensions 40×40 mm and also 20×10 mm (see section 5) are illustrated in the Figure 4.

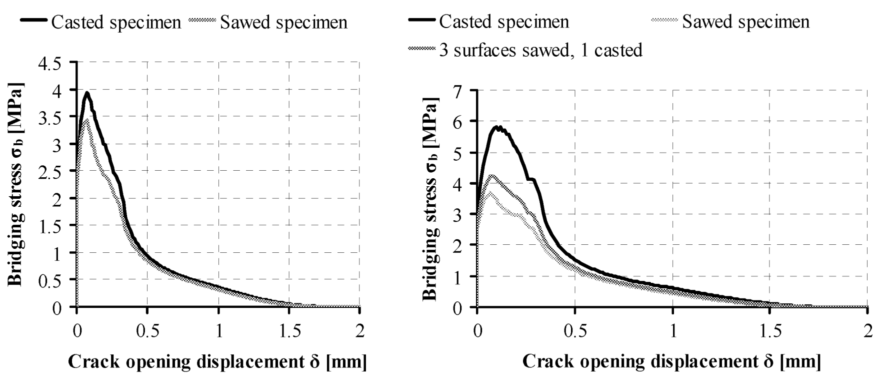

Fig.4: Typical $\sigma_b(\delta)$ relations for specimens reinforced with fibers with $L_f = 12$ mm over the whole cross-sectional plane (40×40 mm left, 20×10 mm right)

Figure 5 shows the maximum bridging stress $\sigma_{\mathrm{mb}}^{kl}$ for specimens (with dimensions 40×40 mm) reinforced by fibers with $L_{\mathrm{f}} = 12$ mm and divided by the grid with $d_{\mathrm{x}} = 4$ mm. In the case of casted specimen, surface layer has a higher maximum bridging stress than the core. The highest strength is calculated in corner sections where the fibers are aligned with two surfaces and their direction nearly corresponds to the longitudinal axis. In the case of sawed specimen, it is just the opposite. Damaged fibers (with reduced embedment length) are able to transfer reduced force and therefore the surface layer is weakened. It is particularly evident in the corners where the fibers are sawed by both surfaces. Therefore the maximum bridging stress from the whole cross-section ($d_{\mathrm{x}} = 40$ mm) is higher for casted specimen than for sawed specimen (Fig. 4). The differences in values are more obvious for specimen with small cross-sectional area (Fig. 4 right), while for large cross-sectional area (Fig. 4 left) it diminishes because thickness of affected layer does not change with changing size of specimens.

Afterwards the cross-sectional area was divided by finer grid with $d_{\mathrm{x}} = 1$ mm. Figure 6 shows the average maximum bridging stress $\sigma_{\mathrm{mb}}^{kl}$ (through the central part) of specimens with different preparation methods and length of fibers. In all cases, inner part of specimen has the

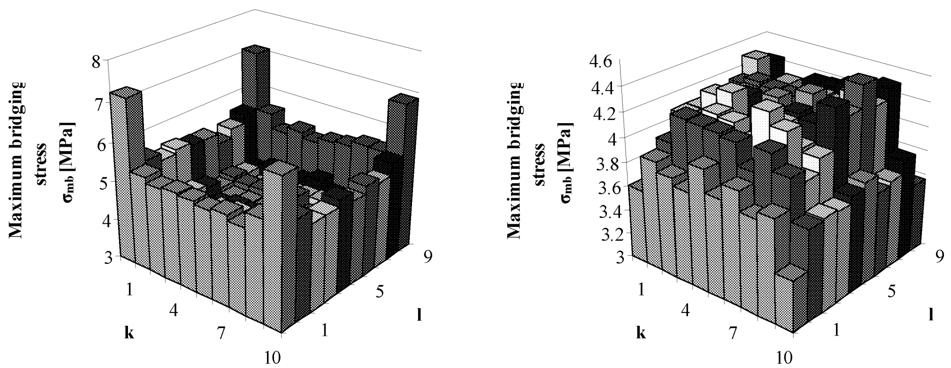

Fig.5: Maximum bridging stress $\sigma_{\mathrm{mb}}^{kl}$ at individual parts of the cross-sectional plane ($d_{\mathrm{x}} = 4$ mm) of casted (left) and sawed (right) specimen

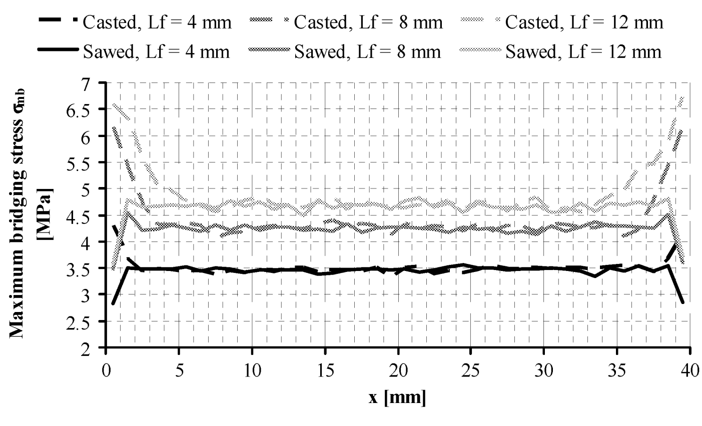

Fig.6: Average maximum bridging stress $\sigma_{\mathrm{mb}}^{kl}$ at individual parts of the the cross-sectional plane ($d_{\mathrm{x}} = 1$ mm) of specimens with different preparation method and length of fibers

same maximum bridging stress for both preparation methods. In the case of sawed specimens the weakened surface layer has similar depth about 1–2 mm for all length of fibers, while in the case of casted specimens the depth of affected layer depends on the length of the fiber and corresponds approximately to the one half of fiber's length. Weakened layer has smaller depth because broken fibers with increasing distance from the surface deflect more from the longitudinal axis and thus contribute less to the overall bridging stress (Eq. (4), (5), (7)).

5. Reproduction of an experiment using numerical simulations

Several years ago, a comparative study organized by RILEM (not published yet) was carried out in order to compare experimental data from tensile tests of engineered cementitious composites ECC performed in different laboratories. All sets were prepared from material with the same composition. Differences were only in their shape, method of preparation and treatment. Two sets were prepared even from the same batch in one lab. These experiments were subsequently numerically simulated using finite element method [5]. The two sets were used for parametric study of material characteristics. In order to capture properly the tensile behavior of both sets, the influence of preparation method had to be considered in calculations. The first set was completely casted, while the second one was casted and then sawed along three surfaces (Fig. 7). Since the calculations were performed in 2D, the effect of damaged fibers was averaged through the specimen thickness, assuming that strength of fiber reinforcement linearly decreased towards cut surface up to distance corresponding to half of fiber length. This simplified assumption reduced stress in cohesive law to 70 % of the original value.

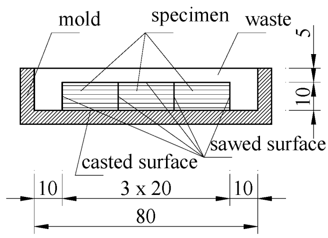

Fig. 7: Schematic drawing of the experimental specimen

If we apply our model for correct distribution and damage of fibers in specimens from second set with cross-sectional area 20×10 mm, we obtain the maximum bridging stress $\sigma_{\mathrm{mb}} = 5.81$ MPa for casted case (Fig. 4 right). In the case of one casted and three sawed surfaces we obtain $\sigma_{\mathrm{mb}} = 4.22$ MPa. That is reduction approximately to 72 % of the original value and it is in very good agreement with the original assumption. It should be noted that the values of maximum bridging stress correspond to the lime matrix reinforced with PVA fibers. We assume that for cementitious composites the ratio of values would be the same.

6. Conclusion

The results of numerical calculations show that the specimens preparation method has to be taken into account during the design and evaluating of experiments. It was demonstrated, that the strength of fiber reinforcement in surface layer of sawed specimens is weakened due to damage of fibers. While in the case of casted specimens, fibers tended to align with mold surface and thus the maximum bridging stress in surface layer is higher. The results show that the depth of weakened surface layer doesn't depend on the fiber length compared to the depth of the reinforced layer in the case of casted specimens.

Acknowledgement

The presented research has been carried out with financial support of the Czech Technical University in Prague under project SGS13/034/OHK1/1T/11.

References

[1] Li V.C., Leung C.K.Y.: Steady state and multiple cracking of short random fiber composites. Journal of Engineering Mechanic, 118, 11 (1992) p. 2246–2264
[2] Yang E.-H., Wang S., Yang Y., Li V.C.: Fiber-Bridging Constitutive Law of Engineered Cementitious Composites, Journal of Advanced Concrete Technology, 6, 1 (2008) p. 181–193
[3] Přinosil M., Kabele P.: Prediction of the behavior of lime mortar reinforced with fibers based on their micromechanical parameters, In: J. Jasieńko (ed.) Proceedings of the International Conference on Structural Analysis of Historical Constructions, Wroclaw University of Technology, Wroclaw 2012, p. 883–889
[4] Přinosil M.: FiberBridging: User's manual [online], [cited 2013-07-22], available from: http://mech.fsv.cvut.cz/ prinosil/index.php?id=FiberBridging, (2012)
[5] Přinosil M.: Modeling of Fiber Reinforced Cementitious Composites using Stochastic Finite Elements, Master's thesis, Czech Technical University in Prague, Prague 2010

Received in editor's office: September 9, 2013
Approved for publishing: February 22, 2014